

Evaluation of temperature changes in a cell culture plate well with absorbing walls containing a 3D model of tumour spheroid under irradiation in the optical range

N.V. Sapogova, D.V. Yuzhakova, A.A. Smirnov, M.V. Shirmanova, M.M. Lukina, A.I. Gavrina, A.V. Izosimova, E.V. Zagaynova, V.A. Kamensky

Abstract. The temperature conditions for photodynamic therapy of the culture of tumour cells organised in 3D spheroids are studied. The spheroids are placed in the cell culture medium in the well of a special cell culture plate with absorbing walls. A mathematical model is presented that describes the temperature distribution in a well with a cell culture plate heated by optical radiation. It is shown that the temperature in the well volume is not uniformly distributed, and the temperature on the well surface can differ significantly from the temperature in its volume.

Keywords: photodynamic therapy, 3D tumour spheroids, thermal conductivity, effect of laser radiation on a tumour.

Photodynamic therapy (PDT) is a clinically approved, minimally invasive therapeutic method for the destruction of target cells under the influence of radiation. The method is based on the accumulation of phototoxic drugs, i.e. photosensitisers, in the focus of the disease, which, when excited by light with a certain wavelength, generate active forms of oxygen that are toxic to living cells [1, 2]. Currently, PDT is widely used to treat malignant neoplasms, in particular, various types of cancer of skin and hollow internal organs, as well as some nononcological diseases [3]. Despite significant progress in the field of PDT cancer treatment, there is still a huge field for research as well as active development of new photosensitisers and tumour irradiation regimes.

N.V. Sapogova, A.A. Smirnov, V.A. Kamensky Federal Research Center Institute of Applied Physics of the Russian Academy of Sciences, ul. Ulyanova 46, 603950 Nizhny Novgorod, Russia; e-mail: ns@ufp.appl.sci-nnov.ru; vlad@ufp.appl.sci-nnov.ru;
D.V. Yuzhakova, M.V. Shirmanova, M.M. Lukina, A.I. Gavrina Privolzhsky Research Medical University, pl. Minina i Pozharskogo 10/1, 603005 Nizhny Novgorod, Russia; e-mail: yuzhakova-diana@mail.ru;
A.V. Izosimova Privolzhsky Research Medical University, pl. Minina i Pozharskogo 10/1, 603005 Nizhny Novgorod, Russia; Lobachevsky State University of Nizhny Novgorod, prosp. Gagarina 23, 603950 Nizhny Novgorod, Russia;
E.V. Zagaynova Lobachevsky State University of Nizhny Novgorod, prosp. Gagarina 23, 603950 Nizhny Novgorod, Russia

A standard stage in the development of new approaches to PDT of tumours is *in vitro* study on a monolayer culture of tumour cells or on 3D tumour spheroids [4–7]. According to the generally accepted technique, the irradiation of tumour cells is carried out in cell culture plates with absorbent walls made of black opaque plastic to minimise light rescattering [8, 9]. However, in the course of irradiation, a significant increase in the temperature of the medium in the wells with tumour cells can occur, giving rise to the development of hyperthermal reactions in the irradiated cells, which can lead to an incorrect interpretation of the therapy results. In most studies, temperature changes during irradiation are monitored on the surface of the medium in the well. Obviously, the temperatures in the volume of the well and on its surface can differ significantly, which should be taken into account in the experiment. Although the calculations of the temperature distribution in biological media have already been performed earlier [10], this configuration of a biological experiment has become relevant only recently.

The aim of the presented work was to construct a mathematical model that allows temperature changes to be calculated in the entire volume of a cell culture plate well with black opaque walls under exposure to optical radiation.

We studied 3D tumour spheroids formed from the cells of the human cervical cancer HeLa Kyoto line. Tumour spheroids are microaggregates of spherical tumour cells. They are an extremely convenient model for research, because, on the one hand, they are closer in their properties to real tumours than a monolayer cell culture, and on the other hand, they are easy to use. Spheroids were cultivated in a nutritive medium DMEM (Dulbecco's Modified Eagle Medium, PanEko, Russia) containing phenol red to monitor its pH and, therefore, the state of the spheroids. Irradiation and visualisation of spheroids were performed in a colourless DMEM medium without phenol red (Gibco, United States), whose background fluorescence is minimal. To irradiate tumour spheroids, an Epistar LED (Taiwan) with a centre wavelength of $\lambda = 465$ nm was used. The spheroids were located at the bottom or in the middle of the cuvette in height. The temperature on the well surface during the experiment was measured using an Optris PI400 thermal imager (Optris GmbH, Germany).

Within the framework of this work, we reveal to what extent the temperature at the surface, determined experi-

mentally, corresponds to the temperature in the bulk of the liquid. For this purpose, it is necessary to solve the problem of thermal conductivity in the system under consideration. In the calculations, we assume that the liquid medium fills the edges a cylindrical well of the plate with a depth of $H = 1$ cm and an inner diameter of $D = 6.5$ mm. The well wall thickness is 0.7 mm. Consider the heating of a medium exposed to radiation at a wavelength of 465 or 630 nm. Irradiation at a wavelength of 630 nm is standard for PDT of tumours [11], while calculation at a wavelength of 465 nm is necessary to work with the phototoxic miniSOG protein [6]. The radiation passes through the aperture, which coincides with the inner diameter of the well and is located directly at its upper boundary, has a large divergence angle $\sim 120^\circ$, which is typical for superluminescent diodes, and is maximally absorbed by the walls of the well.

Measurements showed that the absorption coefficient μ_{las} of the colourless culture DMEM medium without phenol red is 0.1 cm^{-1} at a wavelength of 465 nm. The absorption coefficient of the standard DMEM culture medium with phenol red changes due to the addition of an acid-base indicator and is 0.67 cm^{-1} at a wavelength of 465 nm. At a wavelength of 630 nm, both DMEM media, colourless and with phenol red, are practically transparent, and their absorption coefficients are 0.016 and 0.026 cm^{-1} , respectively.

In the calculations, we will assume that tumour spheroids do not differ in their optical properties from a liquid medium, i.e., the absorption coefficient of spheroids coincides with the absorption coefficient of the medium and there is no radiation scattering on them.

The walls of the plate are opaque at the wavelengths under consideration. For calculations, the absorption coefficient of the wall material was taken such that 99% of the radiation was absorbed by the well wall. The bottom of the plate is made of transparent plastic, the absorption of which was neglected.

The calculations took into account the cooling of the walls of the well and the free surface of the liquid medium because of heat exchange with air at room temperature.

The temperature distribution in the medium is described by the heat conduction equation

$$\frac{\partial T}{\partial t} = \alpha \Delta T + \frac{f}{c\rho}, \quad (1)$$

where T is the temperature of the environment; α is the coefficient of temperature conductivity of the medium; c and ρ are the specific heat and density of the medium, respectively; and f is the heat source intensity. Since the system under consideration has a cylindrical symmetry, the calculation is performed in coordinates (r, z) , where r is the distance from the axis, and z is the distance from the well surface.

Let us specify f in Eqn (1) as

$$f = f_0 \left[1 + \frac{z \tan(\beta/2)}{R} \right]^{-2} \exp\left(-\int_0^{l(r,z)} \mu dl\right). \quad (2)$$

Here f_0 determines the radiation intensity on the liquid surface in the well at $z = 0$; $R = 3.25$ mm is the inner radius of the well. In the experiment, the central part of the beam was used as a radiation source, and the beam edges were cut off

by an aperture, whose diameter coincided with the inner diameter of the well. The experimentally measured profile of the beam central part showed that $f_0(r) \approx \text{const}$. The coefficient $[1 + z/R \tan(\beta/2)]^{-2}$ allows estimating the decrease in beam intensity due to its divergence as the ratio of the initial area of the beam at the entrance to the area that the beam would occupy propagating in a liquid at depth z in the absence of well walls. The exponential factor in Eqn (2) is responsible for the attenuation of radiation due to absorption when passing the path $l(r, z)$; here the absorption coefficient $\mu = \mu(r, z)$ is a function of coordinates, since the absorption coefficients in the liquid and in the material of the well walls are different.

At the outer boundaries of the well and at the free surface of the liquid, taking into account heat exchange with air yields the following boundary conditions:

$$k \frac{\partial T}{\partial n} + U(T - T_{\text{room}}) = 0, \quad (3)$$

where $k = \alpha c \rho$ is the thermal conductivity coefficient; U is the heat transfer coefficient of the corresponding medium; T_{room} is the room temperature; and $\partial/\partial n$ is the derivative taken along the normal to the surface. We will assume that the condition of perfect thermal contact is fulfilled at the inner boundaries, i.e., the temperature and the heat flux are continuous.

Under the conditions of the considered geometry, the averaged coefficient of radiation reflection from the upper part of the well walls (the region from the surface to half the depth of the well) is small, namely, it does not exceed 2.5%, which makes this effect negligible. Closer to the bottom of the well, the reflection coefficient increases. The small fraction of radiation incident on the inner surface of the lower half of the well (not more than 10%) makes it possible not to consider the effect of radiation reflection from the walls in the entire volume of the well.

In the calculations, we take into account that in biological media there is a critical maximum temperature $T_{\text{crit}} = 43^\circ\text{C}$ [12], the excess of which leads to the development of hyperthermal reactions in irradiated cells; considering these reactions is beyond the scope of PDT. At $T_{\text{room}} = 20^\circ\text{C}$ this means a maximum heating of 23°C .

Since the culture medium and the spheroid consist mainly of water, we assumed their physical characteristics to be equal to the corresponding characteristics of water. Namely, we assumed that the density, heat capacity and thermal conductivity of the liquid and the spheroid are as follows: $\rho = 1 \text{ g cm}^{-3}$, $c = 4.2 \text{ J g}^{-1} \text{ K}^{-1}$ and $k = 6 \times 10^{-3} \text{ W cm}^{-1} \text{ K}^{-1}$ [13]. For the material of the well walls (polystyrene), the following parameters were used: $c_w = 1.11 \text{ J g}^{-1} \text{ K}^{-1}$, $\rho_w = 1.1 \text{ g cm}^{-3}$, and $\alpha_w = 10^{-3} \text{ cm}^2 \text{ s}^{-1}$ [14]. The polystyrene/air heat transfer coefficient is $U_w = 8 \text{ W m}^{-1} \text{ K}^{-1}$, which corresponds to a gas with free convection [15].

The liquid/air heat transfer coefficient U_{las} significantly depends on the experimental conditions. To determine the U_{las} value, the temperature of the liquid surface was measured under exposure at two different optical radiation powers. This allowed estimating the U_{las} value, which was $\sim 45 \text{ W m}^{-2} \text{ K}^{-1}$. Experimental data and calculation results are shown in Fig. 1.

Numerical calculations were carried out on a rectangular grid using the alternating direction method.

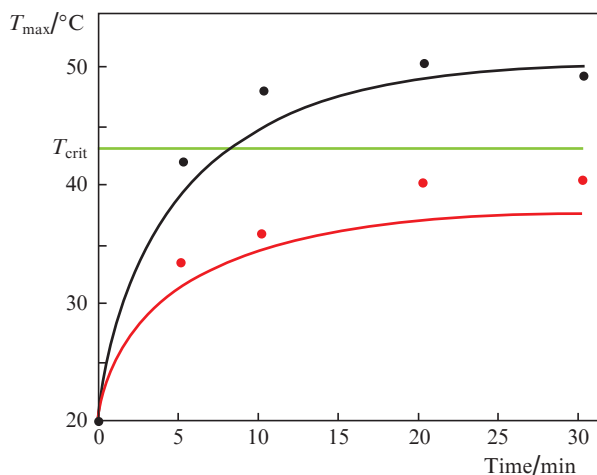


Figure 1. (Colour online) Experimental (dots) and calculated (curves) time dependences of the maximum temperature T_{\max} of heating the liquid surface upon exposure to a LED with a central wavelength of 465 nm at an optical power of 129 mW (black curves and dots) and 75 mW (red curves and dots).

Using the obtained estimate of the heat transfer coefficient U_{las} , the temperature distribution in the considered sample was calculated after 30 min of irradiation with a power of 75 mW at wavelengths of 465 and 630 nm. The results are shown in Fig. 2 for colourless and phenolic red DMEM media at 465 and 630 nm. Since these media are practically transparent at a wavelength of 630 nm, the temperature distribution pattern for them is the same. In the figures, the circle denotes a spheroid with a diameter of 500 μm to understand the spheroid scale compared to the cuvette size. The position of the spheroid is conditionally selected in the centre of the well at a height of 2 mm from the bottom.

Figure 3 shows the change of the maximum temperature on the liquid surface (bold lines) and in the region of the con-

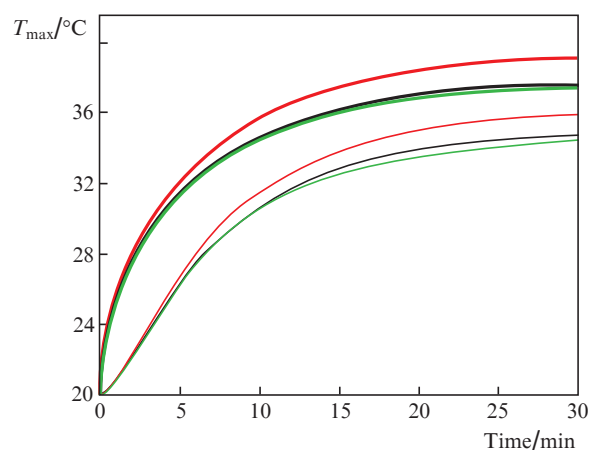


Figure 3. (Colour online) Time dependences of the maximum temperature attained on the surface of the medium (thick lines) and in the conditional region of the spheroid location (thin lines) under exposure to 75-mW radiation: colourless DMEM medium, $\lambda = 465$ nm (black curves), medium DMEM with phenol red, 465 nm (red curves), colourless DMEM and DMEM with phenol red, 630 nm (green curves).

ditional location of the 3D spheroid indicated in Fig. 2 by a black circle (thin lines) during irradiation.

Figure 2 shows that during irradiation a depth-inhomogeneous temperature distribution is formed in the medium. The maximum heating occurs near the surface due to absorption of radiation by the well walls. In the depth of the well, closer to the bottom, the temperature of the liquid decreases. The temperature distribution pattern in the medium is almost the same in all considered cases. However, when a phenolic red DMEM medium is irradiated at a wavelength of 465 nm, a stronger heating is observed and the maximum temperature exceeds room temperature by $\sim 8\%$. This is due to the significant absorption by the phenol red liquid at a wavelength of 465 nm.

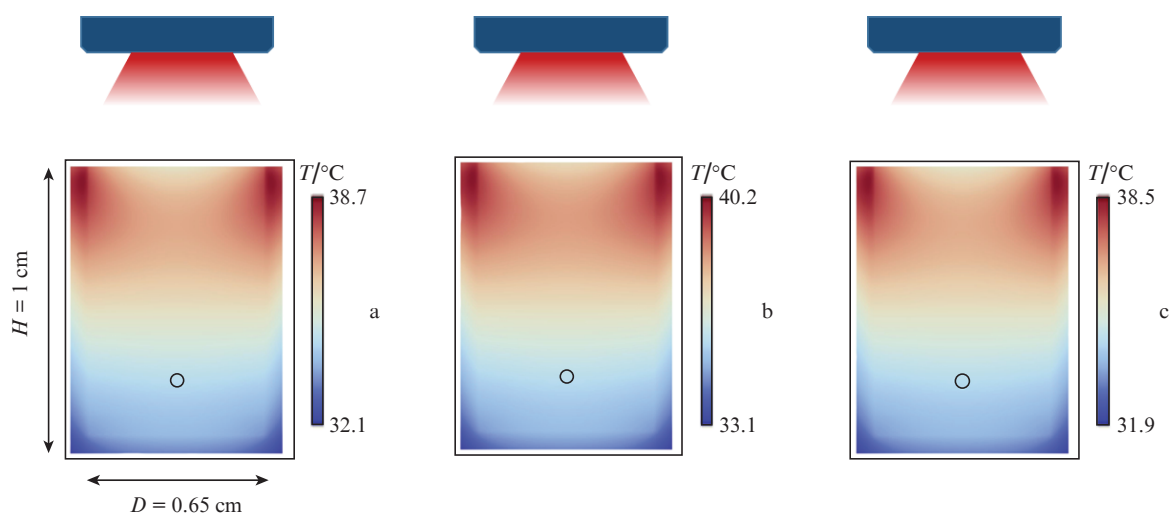


Figure 2. (Colour online) Temperature distribution in the sample after 30 min irradiation at a power of 75 mW: (a) colourless DMEM medium, $\lambda = 465$ nm, (b) DMEM medium with phenol red, 465 nm, (c) colourless DMEM and DMEM with phenol red, 630 nm. The circle denotes the area of the spheroid conditional localisation.

The difference between the maximum temperature rise above the room temperature on the surface of the liquid and in the region of conditional localisation of the 3D spheroid (the region of the spheroid position is indicated in Fig. 2 by a black circle) is $\sim 16\%$. When carrying out experiments with medium heating by irradiation, it is necessary to take into account the fact that the temperature of the medium surface, measured with a thermal imager, can differ significantly from the temperature in the depth of the medium, in the area where the tumour spheroids are located. This is of particular importance for tasks in which it is needed to heat spheroids to a certain temperature, not exceeding T_{crit} .

The performed theoretical calculations were tested on 3D tumour spheroids. For this purpose, samples containing spheroids in a culture medium were irradiated for 20 min with radiation with a power density of 75 mW cm^{-2} at a wavelength of 465 or 630 nm. According to the calculations performed earlier (Fig. 3), the heating of the medium achieved in the well of the cell culture plate under such modes of exposure does not exceed the critical values and should not lead to hyperthermal reactions.

Normally, a spheroid consists of the central core and the peripheral layer (Figs 4a and 4c). The dense dark central zone is mainly dead necrotic cells that have died due to hypoxia and insufficient supply of nutrients to the central zone, and the lighter peripheral layer is mostly living, actively dividing

cells. Normally, tumour spheroids may slightly differ from each other due to natural biological diversity.

In Figs 4a and 4c, bright-field and fluorescent images of tumour spheroids are shown without exposure to laser radiation, and in Figs 4b and 4d, of spheroids irradiated for 20 min with laser radiation with a power density of 75 mW cm^{-2} at wavelengths of 465 or 630 nm, respectively. As seen in the bright-field images, the spheroids after irradiation, as well as the control (unirradiated) spheroids consist of a dark central core and a lighter peripheral zone.

To verify the viability of tumour cells in the composition of a spheroid, they were stained using a set of fluorescent dyes Apoptosis/Necrosis detection kit (Abcam, UK). The dye CytoCalcein Violet 450 binds to the cytoplasm of living cells (the blue channel in fluorescence images). The dye 7-amino-actinomycin D binds to the nucleus of damaged dead cells and serves as a necrosis marker (the green channel in fluorescent images). Fluorescent images in Fig. 4 are a superposition of two channels. It can be seen that the dark necrotic nucleus corresponds to the green zone of dead cells, in which there is a certain amount of living cells, while the lighter peripheral layer corresponds to the blue zone of living cells, in which there are single dead cells.

A comparative analysis of the control unirradiated and irradiated spheroids showed that irradiation with a power density of 75 mW cm^{-2} for 20 min at a wavelength of 465 or

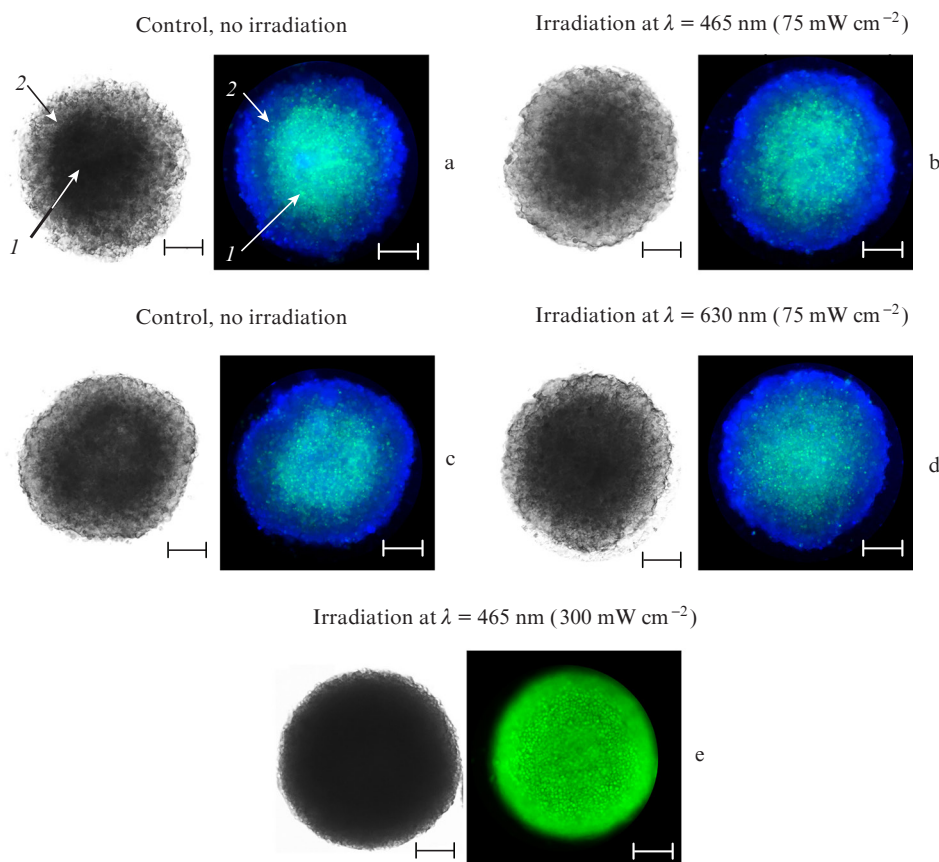


Figure 4. (Colour online) Microscopic images of HeLa Kyoto tumour spheroids. For each spheroid, two images are presented: on the left, obtained using bright field microscopy; on the right, using fluorescence microscopy. The blue channel shows viable cells, the green channel demonstrates dead necrotic cells. The arrows mark the spheroid zones: (1) dark necrotic nucleus, (2) light peripheral layer of living cells; (a, c) control, unirradiated, spheroids, (b, d) spheroids after irradiation with a power density of 75 mW cm^{-2} for 20 min at a wavelength of 465 or 630 nm, respectively, (e) a spheroid after irradiation with a power density of 300 mW cm^{-2} . The scale bar corresponds to 170 microns. To obtain fluorescent images, staining was carried out after irradiation.

630 nm has no negative effect on the spheroids. Their shapes, as well as the ratio of the zones of living and dead cells in the irradiated spheroids, do not generally differ from the control ones. The insignificant differences are explained by the fact that normally unexposed spheroids also differ insignificantly from each other. Thus, it is experimentally confirmed that there are no thermal effects when 3D spheroids are irradiated at a power density of 75 mW cm^{-2} .

For comparison, Fig. 4e shows a spheroid irradiated at a power density of 300 mW cm^{-2} at a wavelength of 465 nm. In this case, according to calculations, the medium is heated to a temperature substantially higher than T_{crit} , which should lead to a hyperthermal reaction. Figure 4e shows that the structures of the irradiated and unirradiated spheroids are significantly different. Almost the entire volume of the irradiated spheroid is a dense dark mass of dead cells (bright field image) bound to the 7-aminoactinomycin D dye and visualised in the green channel (fluorescent image). The bright-field image lacks the light peripheral layer of living cells and, accordingly, the blue zone in the fluorescent image. Thus, in this case, a hyperthermal reaction is clearly demonstrated.

Experimental studies have shown that the theoretical model considered in this work allows adequate determination of the temperature in the sample when it is exposed to optical radiation and to assess the possibility of the hyperthermal reactions in tumour spheroids. According to the considered model, the temperature in the volume of the well is not uniformly distributed, and its value on the surface can differ significantly from the value in the volume of the well.

Acknowledgements. The work was supported by the Ministry of Science and Higher Education of the Russian Federation within the framework of the State Assignment of the Institute of Applied Physics of RAS (Project No. 0035-2019-0012) and the Russian Foundation for Basic Research (Grant No. 18-42-520027 r_a).

References

1. Agostinis P., Berg K., Cengel K.A., Foster T.H., Girotti A.W., Gollnick S.O., Hahn S.M., Hamblin M.R., Juzeniene A., Kessel D., Korbelik M., Moan J., Mroz P., Nowis D., Piette J., Wilson B.C., Golab J. *CA Cancer J. Clin.*, **61**, 4 (2011).
2. Allison R.R., Moghissi K. *Clin. Endosc.*, **46**, 1 (2013).
3. Van Straten D., Mashayekhi V., de Bruijn H.S., Oliveira S., Robinson D.J. *Cancers (Basel)*, **9**, 2 (2017).
4. Austin E., Jagdeo J. *J. Vis. Exp.*, **138**, 58190 (2018).
5. Gao R., Mei X., Yan D., Liang R., Wei M. *Nat. Commun.*, **9**, 2798 (2018).
6. Ryumina A.P., Serebrovskaya E.O., Shirmanova M.V., Snopova L.B., Kuznetsova M.M., Turchin I.V., Ignatova N.I., Klementieva N.V., Fradkov A.F., Shakhov B.E., Zagaynova E.V., Lukyanov K.A., Lukyanov S.A. *Biochim. Biophys. Acta*, **1830**, 11 (2013).
7. Kuznetsova D.S., Shirmanova M.V., Dudenkova V.V., Subochev P.V., Turchin I.V., Zagaynova E.V., Lukyanov S.A., Shakhov B.E., Kamensky V.A. *J. Biophoton.*, **8**, 11 (2015).
8. Gavrina A.I., Shirmanova M.V., Aksenova N.A., Yuzhakova D.V., Snopova L.B., Solovieva A.B., Timashev P.S., Dudenkova V.V., Zagaynova E.V. *J. Photochem. Photobiol. B*, **178**, 614 (2018).
9. Yuzhakova D.V., Lermontova S.A., Grigoryev I.S., Muravieva M.S., Gavrina A.I., Shirmanova M.V., Balalaeva I.V., Klapshina L.G., Zagaynova E.V. *Biochim. Biophys. Acta.*, **1861**, 12 (2017).
10. Stureson C., Andersson-Engels S. *Phys. Med. Biol.*, **40**, 2037 (1995).
11. Stranadko E.F. *Lazernaya Meditsina*, **6**, 1 (2002).
12. Dewey W.C. *Int. J. Hyperthermia*, **10**, 4 (1994).
13. Grigoriev I.S., Meilikhov E.Z. (Eds) *Handbook of Physical Quantities* (Boca Raton: CRC Press, 1997; Moscow: Energoatomizdat, 1991).
14. Novichenok L.N., Shul'man Z.P. *Teplofizicheskie svoystva polimerov* ((Thermophysical Properties of Polymers) (Minsk: Rabota i tekhnika, 1971) p. 120.
15. www.thermopedia.com/content/840.